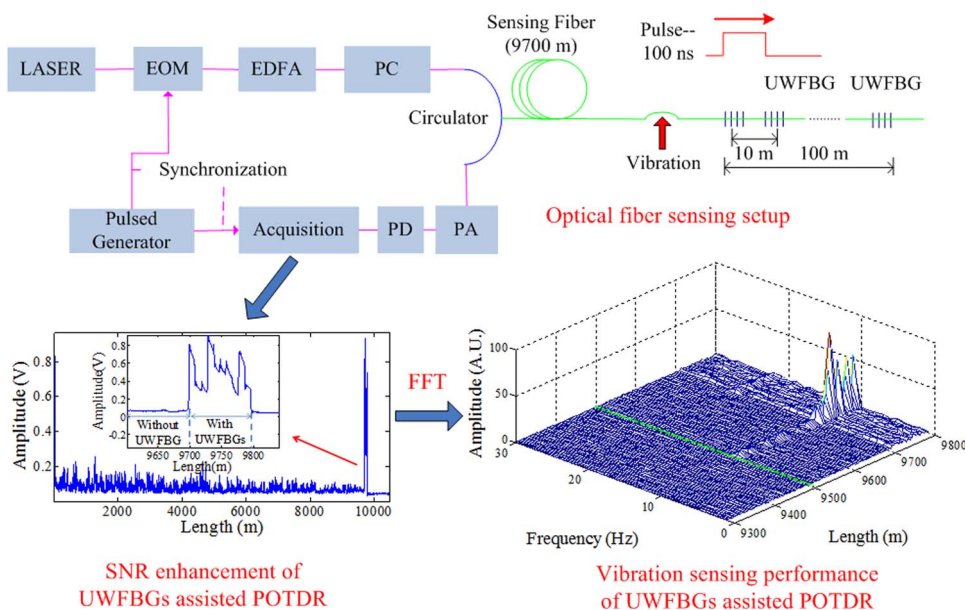🔓 **Open Access**

SNR Enhanced Distributed Vibration Fiber Sensing System Employing Polarization OTDR and Ultraweak FBGs

Volume 7, Number 1, February 2015

Xiangchuan Wang
Zhijun Yan
Feng Wang
Zhongyuan Sun
Chengbo Mou
Xuping Zhang
Lin Zhang

Optical fiber sensing setup

SNR enhancement of UWFBGs assisted POTDR

Vibration sensing performance of UWFBGs assisted POTDR

SNR Enhanced Distributed Vibration Fiber Sensing System Employing Polarization OTDR and Ultraweak FBGs

Xiangchuan Wang,[1,2] **Zhijun Yan,**[2] **Feng Wang,**[1] **Zhongyuan Sun,**[2] **Chengbo Mou,**[2] **Xuping Zhang,**[1,3] **and Lin Zhang**[2]

[1]Institute of Optical Communication Engineering, Nanjing University, Nanjing 210093, China
[2]Aston Institute of Photonic Technologies, Aston University, Birmingham B4 7ET, U.K.
[3]Key Laboratory of Modern Acoustics, Nanjing University, Nanjing 210093, China

Abstract: A distributed fiber sensing system based on ultraweak FBGs (UWFBGs) assisted polarization optical time-domain reflectometry (POTDR) is proposed for load and vibration sensing with improved signal-to-noise ratio (SNR) and sensitivity. UWFBGs with reflectivity higher than Rayleigh scattering coefficient per pulse are induced into a POTDR system to increase the intensity of the back signal. The performance improvement of the system has been studied. The numerical analysis has shown that the SNR and sensitivity of the system can be effectively improved by integrating UWFBGs along the whole sensing fiber, which has been clearly proven by the experiment. The experimental results have shown that by using UWFBGs with 1.1×10^{-5} reflectivity and 10-m interval distance, the SNR is improved by 11 dB, and the load and vibration sensitivities of the POTDR are improved by about 10.7 and 9 dB, respectively.

Index Terms: Fiber optics system, fiber gratings, distributed fiber sensor, optical fiber polarization.

1. Introduction

Polarization optical time domain reflectometry (POTDR) is proposed for single-end distributed fiber sensing and measurement by detecting the state of polarization (SOP) of the propagating pulse via time [1]. It has been widely used in the polarization properties analysis of optical fiber communication system, such as polarization mode dispersion (PMD) [2], polarization dependent loss (PDL) [3], and beat length [4] measurement over the past few decades. Beside the measurement of polarization related communication parameters, POTDR can also be used as an all fiber distributed sensing system [1], [5], [6] due to its advantages such as high sensitivity, short response time, versatile design that can adapt various environments, and so on. Therefore, it can be used for vibration detection, which is really important in perimeter security dynamic monitoring, dam and rail vibration monitoring, *etc.* In an OTDR based distributed sensing system, the performance such as the sensing dynamic range, spatial resolution, and sensitivity are governed by the system signal to noise ratio (SNR), which is limited by the low intrinsic Rayleigh scattering

(RS) coefficient of the optical fiber [7]. Increasing the sensing dynamic range with high spatial resolution and sensitivity is therefore highly desirable in a practical term. So far, three main methods have been proposed to improve SNR in an OTDR-based system. A very much intuitive method is to improve the detector sensitivity. For example, a superconducting nanowire based single-photon detector with higher sensitivity has been proposed to integrate in the OTDR system and achieved 22 dB dynamic range with spatial resolution of 6.2 cm [8]. However, with a high sensitivity detector, poor thermal stability and long measurement time have always been big issues. Another approach is based on light source encodings, which could increase the probe light power without inducing nonlinear effect [9], [10]. The third method involves data processing techniques such as frequency transform and wavelet transform to reduce noise [5], [11].

Recently, another approach to improve the SNR by simply improving the back reflectivity signal from single mode fiber (SMF) using fiber Bragg grating (FBG) devices has been proposed. As an effective in-fiber mirror, FBGs have been intensively studied over the past few decades in optical communication systems [12], [13], fiber lasers [14], [15], and fiber sensors [16], [17]. Lo *et al.* have introduced a pair of FBGs into an OTDR system with dual light sources for bend sensing, where the SNR, sensing range and stability were greatly improved due to the enhanced reflection from the FBGs [18]. A large capacity sensing network with weak FBGs multiplexing was achieved by combining OTDR, weak FBGs and wavelength division multiplexing (WDM) techniques [19]. However, these systems are only used for key-positions monitoring [20]–[23]. Moreover, these traditional FBGs-integrated systems are hard to be used for vibration detection due to the long response time. By introducing relatively weak FBGs into an SMF-based POTDR system, Ming *et al.* have demonstrated distributed bend sensing by measuring beat length of SMF with improved SNR [24]. However, it is still difficult to detect vibration using the above mentioned system due to the slow response speed of beat length measurement. In this report, we propose and demonstrate an SNR enhanced distributed sensing system based on ultra-weak FBGs (UWFBGs) associated POTDR which can be used for load and vibration sensing with improved sensitivity. Moreover, the proposed system is able to perform the true distributed sensing function.

The article has been organized as following. First, the principle of the sensing system is presented. We have also simulated the UWFBGs based sensing system using Muller matrix and waveplate model. Then, an experimental POTDR sensing system was constructed to confirm the improvement on SNR and sensitivity. In the system, UWFBGs, whose reflectivity is two orders higher than Rayleigh scattering coefficient of 1-m SMF, are specially designed and fabricated along the fiber sensing network with certain interval distance. Once the spatial resolution equals to the separation of UWFBGs, the detected signal will be the summation of both the UWFBG reflected signal and the back Rayleigh scattering within one pulse at each moment. Then, the amplitude of received signal will be stronger than that of the traditional POTDR along the whole fiber. Therefore the SNR is improved along the whole sensing fiber with UWFBGs in our system due to the enhanced back-reflected signal level. Load and vibration sensing experimental results are also given to show the sensitivity enhancement. Finally, we discuss the limitations of the proposed system and future work followed by the conclusion.

2. Principle and Numerical Simulation

In a standard POTDR system, when the launched pulse travels along the sensing fiber, a back RS signal is generated while the pulse propagates. Then the back RS along the sensing fiber are detected via time. Because the state of polarization (SOP) of the RS is dependent on the birefringence of the sensing fiber experienced by the pulse, the disturbance along the optical fibers which affects the fiber birefringence can therefore be detected by monitoring the change of the SOP of the back RS. Furthermore, the location of the disturbance can also be retrieved via time, achieving distributed fiber sensing [1]. When UWFBGs are introduced into the sensing fiber with certain interval, the detected signal contains not only the back RS but the back signal reflected by UWFBGs as well. Thus, the signal from the UWFBG-based POTDR is larger than
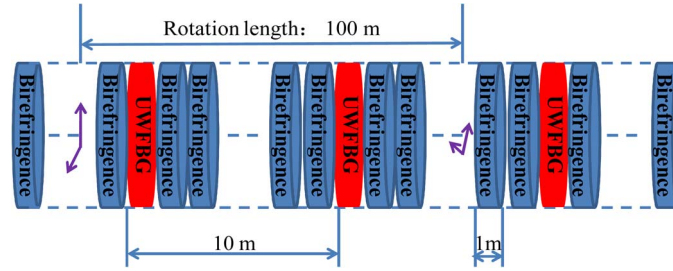
Fig. 1. Waveplate model of sensing fiber with UWFBGs.

TABLE 1

Parameters used in the simulation

Symbol	Parameter	Quantity
L_B	Beat Length	R(40)
L	Fiber Length	10 km
L_I	Interval of UWFBGs	10 m
L_R	Rotation length	100 m
θ	Birefringence angle	$\mu(0,\pi)$
B_c	Circular birefringence	0
R	UWFBG reflectivity	10^{-5}
R_C	Rayleigh scattering coefficient	10^{-7} /m
f	Vibration frequencies	9.2, 10, 11 Hz
α	Attenuation of the SMF	0.2 dB/km
α_{UWF}	Insertion loss of UWFBG	$10\times lg(1\text{-}R)$

R(40) is a Rayleigh-distributed variable with mean value: 40 m [26];
$\mu(0,\pi)$ is the random variable with a uniform distribution between 0
and π, θ_i and θ_j are statiscally independent, whenever i≠j.

the signal from the traditional POTDR. By adjusting the pulse width, we match the pulse width with the interval of UWFBGs to ensure that the back signal contains the back RS and UWFBGs reflected signal at each moment. Then, the signal enhancement can be achieved continuously along the sensing fiber.

The SOP of the probe light would change randomly along the fiber due to the intrinsic birefringence. Thus it is difficult to obtain a straight forward relationship between the SOP of back signal and the disturbance outside. In our simulation, we used Muller matrix and waveplate model [25] to analyze the SOP variation in the SMF and the SNR improvement of the system. The waveplate model is shown below in Fig. 1, by which the fiber is regarded to consist of thousands of birefringence and UWFBG waveplates. In the model, each waveplate is assumed to be 1 m long, and UWFBGs are distributed along the SMF with a 10-m interval distance.

The total matrix (forward, reflection and backward) of the system can be written as

$$S_o = R_1 R_2 \cdots R_{UWF1} \cdots R_j R_{UWFm} \cdots R_N T_N \cdots T_{UWFm} T_j \cdots T_{UWF1} \cdots T_2 T_1 S_1 \qquad (1)$$

where S_i and S_o are the SOP of the input and output light, and T_j and R_j are the forward and backward matrix for the jth birefringence waveplate [25]. T_{UWFm} and R_{UWFm} are the forward and backward matrix of mth UWFBGs. N is the number of total waveplates. For each matrix of waveplate, the intrinsic attenuation and insertion loss induced by UWFBGs are also taken into consideration. The parameters used in the simulation are listed in Table 1.
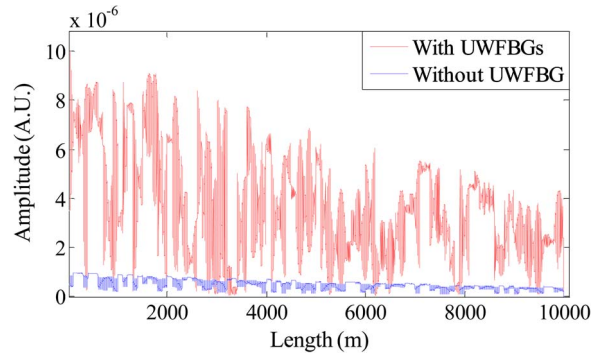
Fig. 2. Simulated POTDR signals with and without UWFBGs using 100 ns pulse.

The simulated POTDR signals of the proposed system with and without UWFBGs are shown in Fig. 2. It can be seen that the amplitude of the POTDR signal fluctuating along the fiber attenuates gradually due to the intrinsic birefringence and loss of the fiber. It is also very clear to see that the signal generated from the POTDR with UWFBGs is much stronger than that without UWFBGs because the detected signal is the sum of one UWFBG reflected signal and 10 m SMF Rayleigh scattering signal at each moment when the spatial resolution is equal to the interval of UWFBGs as shown in Fig. 2. Therefore, the time domain signal could be improved continuously which ensure that the SNR of the system could be improved with no interval along the sensing fiber.

As the POTDR signal fluctuates along the fiber, the amplitude of the fluctuated signal can be used for sensitivity measurement. The power of reflected signal in both POTDR systems is normally less than -30 dBm, the thermal noise dominates in the total noise. Then, the SNR improvement of the UWFBGs assisted POTDR can be determined by

$$\text{SNR}_{\text{improvement}} = \frac{\text{SF}_{\text{C}}}{\text{SF}_{\text{T}}} = \frac{\text{SF}_{\text{UWFBG}} + \text{SF}_{\text{T}}}{\text{SF}_{\text{T}}} = \frac{\text{SF}_{\text{UWFBG}}}{\text{SF}_{\text{T}}} + 1 \qquad (2)$$

where SF_{C} is the signal fluctuation amplitude of the combined system, SF_{T} is the signal fluctuation amplitude of traditional POTDR system, and SF_{UWFBG} is the signal reflected by UWFBG.

Calculation from (2) and Fig. 2 clearly shows that the SNR of the system is improved by about 11 times. As the reflectivity of each UWFBG is about 10^{-5}, the insertion loss of each UWFBG is about 4.3×10^{-5} dB. Therefore, the loss induced by UWFBGs is about 4.3×10^{-3} dB/km (1 km SMF contains 100 UWFBGs in the simulation), which is far less than the round trip loss of the SMF (0.4 dB/km). Therefore, the insertion loss of UWFBG is insignificant to take into consideration and the sensing length can be improved by 10.4 dB$/(0.4$ dB/km$) = 26$ km.

The signal would be reduced due to the loss of the sensing fiber as shown in Fig. 2. When the signal is reduced to the noise level, the corresponding length is defined as sensing length. It is clear to see that the higher the reflectivity of UWFBGs, the better the SNR improvement. However, increasing the reflectivity of UWFBG would increase the loss induced by UWFBG, which may reduce the improvement of sensing length. In the simulation, the relationship between the improved sensing length and the reflectivity of UWFBG was studied and shown in Fig. 3.

As shown in Fig. 3, the improved sensing length increases with the increasing of the UWFBG reflectivity until the reflectivity of UWFBG reaches to -39.2 dB (1.2×10^{-4}). If the reflectivity of UWFBG is further increased, the insertion loss of UWFBG would increase. Then the signal would be reduced much more quickly, which would reduce the improvement of sensing length. Thus, the largest sensing length improvement of the proposed system is about 41.3 km. In this case, the SNR improvement is about 20.8 dB.

The vibration sensitivity improvement is also simulated by assuming 10 UWFBGs integrated fiber connected after 9700 m SMF to be in accord with our experiments. In the simulation, 11 Hz
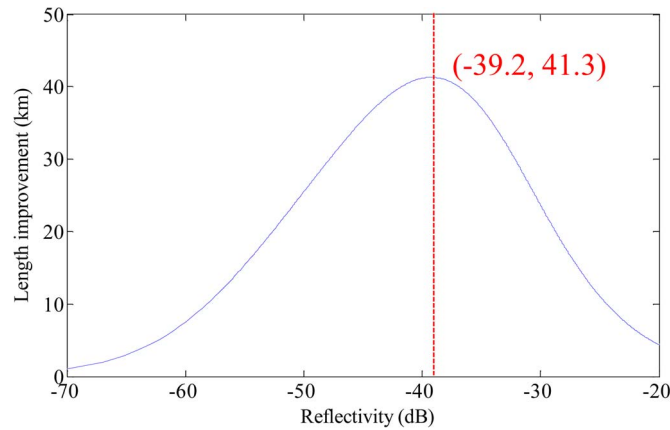
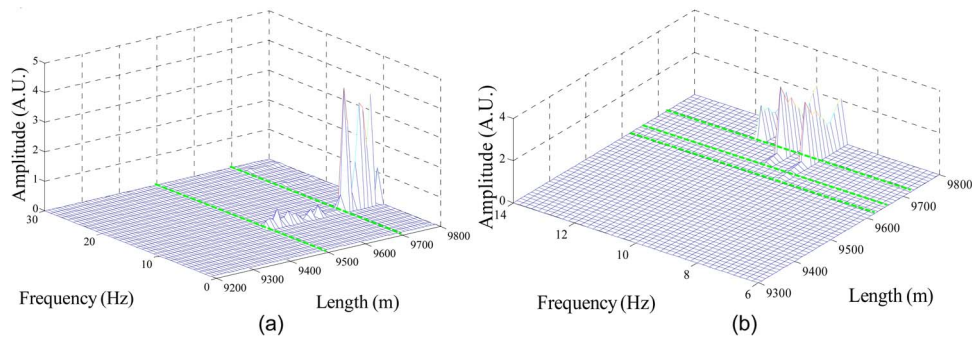Fig. 3. Improved sensing length with different reflectivity of UWFBG.

Fig. 4. Vibration spectra along the fiber. (a) Vibration at 9500 m. (b) Three vibrations at different positions.

vibration was applied at 9500 m, and the signal fluctuation with time was transformed by Fast Fourier Transform (FFT) at each position. Then the spectral distribution along the fiber was obtained and shown in Fig. 4(a). It is shown that the spectra at and after the vibration position all contain 11 Hz because the SOP of the back RS signal generated after the vibration position are all affect by the vibration. Meanwhile the spectra before the vibration position are just noise. Thus, the vibration position can be easily detected by analyzing the spectra along the sensing fiber. The amplitude of 11 Hz frequency component varies along the sensing fiber due to the random birefringence. Because UWFBGs are only inserted between 9700 m and 9800 m while the fiber before 9700 m is SMF, the signal before 9700 m can be used as traditional POTDR signal, and the signal after 9700 m can be used as the enhanced POTDR signal as shown in Fig. 4(a). Thus, the sensitivity improvement can be calculated for about 10 dB by analyzing the amplitude increase of the spectra from the sensing fiber with and without UWFBGs (before and after 9700 m).

Multiple vibrations detection was also studied in the simulation. In accord with the experiments, three vibrations with frequency components of 9.2 Hz, 10 Hz, and 11 Hz were applied at 9630 m, 9665 m and 9725 m, respectively. The spectra along the sensing fiber were obtained as shown in Fig. 4(b). Using the above method, the vibration with frequency components of 9.2 Hz can be easily located at 9630 m. The spectra between 9630 m and 9665 m only contain frequency component of 9.2 Hz while the spectra after 9665 contain the frequency components of 9.2 Hz and 10 Hz. Then, we can judge that another vibration with frequency component of 10 Hz was applied at 9665 m. Similarly, the third vibration with frequency components of 11 Hz can also be located at 9725 m. Thus, distributed multiple vibrations sensing can be achieved. Moreover, comparing the
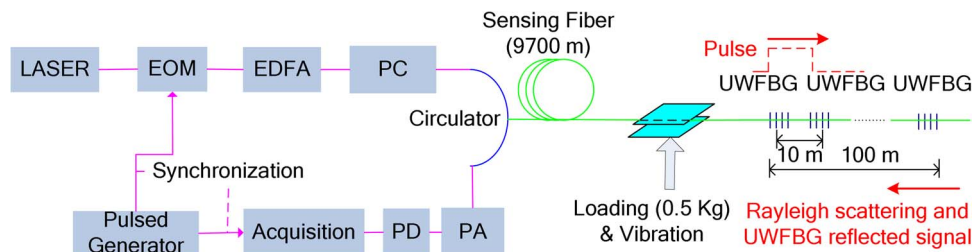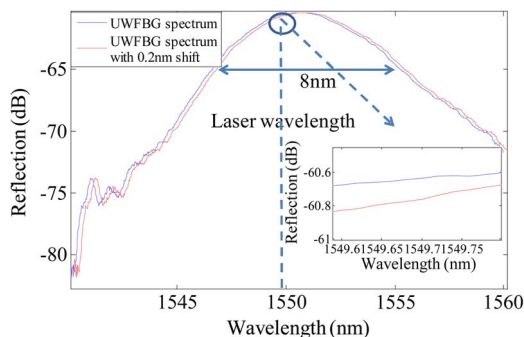
Fig. 5. Hybrid system of POTDR with UWFBGs.

Fig. 6. Reflection spectra of UWFBGs. (Inset) Zoomed spectra near laser central wavelength.

amplitudes of the spectra before and after 9700 m, the SNR of spectra with 9.2 Hz and 10 Hz frequency components were all improved by 10 dB. Thus, the sensitivity of multiple vibrations detection is also improved. In addition, the spectra before the third vibration position have no frequency component related to 11 Hz, especially the UWFBGs region (between 9700 m and 9725 m). Therefore, the introduction of UWFBGs brought no vibration location errors beside the enhancement of sensitivity.

3. Experimental Results and Discussion

3.1. Experimental Setup

The experiment setup of the hybrid system using POTDR with UWFBGs for SNR and sensitivity enhancement in load and vibration detection is shown in Fig. 5. In the proposed system, a CW laser diode with central wavelength at 1549.7 nm is used as the light source. A commercial electro-optic modulator (EOM) with 40 dB extinction ratio is used to generate light pulses. Then the pulse is amplified by an EDFA (IPG Photonics). An in-fiber polarization controller (PC) is employed to change the SOP of the probe light before the pulse is launched into the SMF sensing network. The SOPs of the Rayleigh backscattering and reflected light are converted to electrical intensity signal by a polarization analyzer (PA) and high sensitivity photo-detector (PD). The line-width of the laser is about 0.17 nm. Therefore, the coherent length of the laser is about 1.4 cm, which is much smaller than the pulse width and interval of UWFBGs. Hence, the coherent noise of the system can be ignored.

3.2. UWFBG Characterization and SNR Enhancement Measurement

In the experiment, 10 UWFBGs were UV-inscribed into non-hydrogen loaded SM28 fiber with 10 m separation by using a phase mask exposure method and spliced at the end of 10 km sensing fiber. The length of each UWFBG was around 0.05 mm, which was defined by the UV beam diameter. The measured UWFBG reflection spectrum is shown in Fig. 6. The reflection
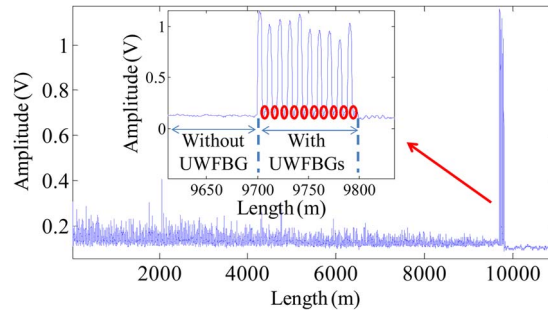
Fig. 7. OTDR signal with 40 ns pulse. (Inset) Zoomed amplitude profile near the UWFBG region.
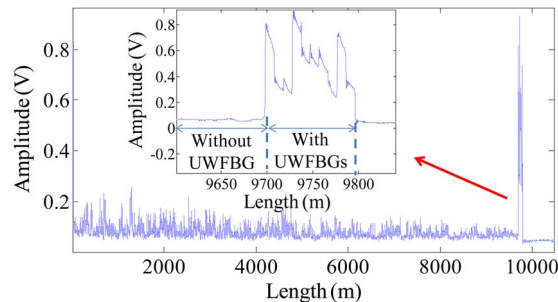

Fig. 8. Detected back reflection signal from the combined POTDR system with 100 ns pulse. (Inset) Zoomed amplitude profile near the UWFBG region.

spectrum of the individual UWFBG is around 1550 nm, covering the wavelength of the input seed laser, and its bandwidth was about 8 nm, which is much wider than laser linewidth, sufficiently eliminating the influence of the spectrum drifting of the UWFBG due to environmental condition (strain, temperature and so on). As shown in Fig. 6, the intensity change caused by 0.2 nm spectral shift (induced by about 15 degrees temperature change) is only about 0.15 dB (3.5%), which is insignificant to the sensor performance.

An OTDR system (taking the PA away from POTDR system in Fig. 5) probed with less than 100 ns pulse was used to show the distribution of UWFBGs and to calculate the reflectivity of UWFBGs in our experiment. In the experiment, 40 ns pulse was chosen. As shown in Fig. 7, 10 UWFBGs are distributed from 9700 m with 10 m interval. The signal from the fiber with UWFBGs is the sum of the Rayleigh scattering and the reflected light of the UWFBG which is one order higher than the signal from the sensing fiber without UWFBG. As the RS coefficient of 4 m SMF is about 4×10^{-7}, the reflected coefficient of the UWFBG can be estimated as $((1.2 - 0.1)/(0.14 - 0.1)) \times 4 \times 10^{-7} = 1.1 \times 10^{-5}$ because the detected signal is improved from 0.04 V (considering the 0.1 V DC signal) to 1.1 V due to the UWFBGs.

As the spatial resolution is less than the interval of UWFBGs when the pulse width is 40 ns, only the signals around UWFBGs were improved as shown in Fig. 7. The signals in the red circle regions in Fig. 7 were still not improved. In this case, the SNR improvement of the proposed system was actually quasi-distributed. When the pulse width was increased to 100 ns, which corresponds to a spatial resolution of 10 m, the signal detected by POTDR is shown in Fig. 8 where the SOP change of the signal is converted to intensity change through the PA in Fig. 5. As UWFBGs interval equals to this spatial resolution, the back reflection signal is the sum of Rayleigh scattering light and the reflected signal from one of the UWFBGs at each moment. Then, the signal is improved continuously along the sensing fiber with UWFBGs. By comparing signals before and after 9700 m, the SNR improvement was estimated to be about 11 dB. Therefore, the sensing length was improved by 11 dB/(0.4 dB/km) $\approx$ 27.5 km.
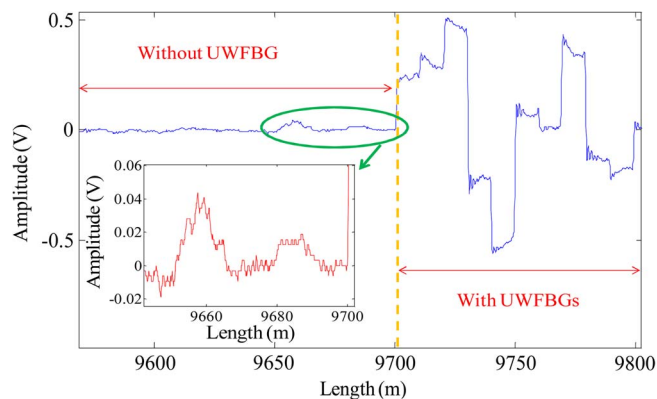
Fig. 9. Load sensitivity of POTDR system. (Inset) Zoomed amplitude profile near the non-UWFBG region, which represents the amplitude profile of traditional POTDR.

3.3. Load Sensing

In this section, the localized load sensitivities of the POTDR system with and without UWFBGs have been investigated. In the experiment, 0.5 kg weight was loaded at the position just before the UWFBG array at 9650 m as shown in Fig. 5. By subtracting the received POTDR signal before loading from the POTDR signal after loading, the signal difference reflects the SOP changes induced by the load. As the SOP of the back RS and UWFBG reflected signal after the load position are all affected by the applied load, the signal difference after 9650 m is changed. We have compared the signals in both regions with and without UWFBGs to show the sensitivity enhancement. As shown in Fig. 9, the SOPs of the lights reflected after 9650 m were all changed while the SOPs of the lights reflected before 9650 m were invariable. Then we can obtain the position information of the load by calculating the start point of the differential signal. The maximum differential signals in non-UWFBG and UWFBGs areas after the load position were used to calculate the sensitivity improvement in our experiment. The maximum differential signals in non-UWFBG area which represents traditional POTDR signal was about 0.042 V, while the change was 0.5 V at 9730 m (with UWFBGs representing enhanced POTDR signal), as shown in Fig. 9. Therefore, the load sensitivity was improved by about 10.7 dB by the UWFBG array in the POTDR system.

3.4. Vibration Detection

Vibrations can also be detected by POTDR system, which is the main application of POTDR due to its fast response speed. The highest frequency of the vibration that can be detected is about 5 kHz for 10 km sensing fiber using POTDR without averaging [5]. However, due to limitation of the vibration loading system in our experiment, vibrations with frequencies around 11 Hz were loaded on the sensing fiber using a mechanical vibration source, which can also be used to show the vibration sensitivity improvement of the proposed system.

Firstly, single vibration with 11 Hz frequency component was applied at 9.5 km in our experiment. The spectra along the fiber are shown in Fig. 10(a). The spectra before 9.5 km have no useful frequency information while the spectra after 9.5 km all contain the frequency components of 11 Hz because the SOP of the back RS and UWFBG reflected signals after the vibration position are all affected. Thus the spectrum and position information of the vibration can be easily obtained by analyzing the spectra along the sensing fiber, achieving distributed vibration sensing. Moreover, as shown in Fig.10(b), 11 Hz can be both detected from the positions without and with UWFBGs which represent the traditional POTDR and the enhanced POTDR respectively. From Fig. 10(a) and (b), it can be seen that the noise at the UWFBGs region was also increased with the signal improvement, which may be caused by the random disturbance along the sensing fiber. Although the noise was also enlarged, the SNR of the spectra with and
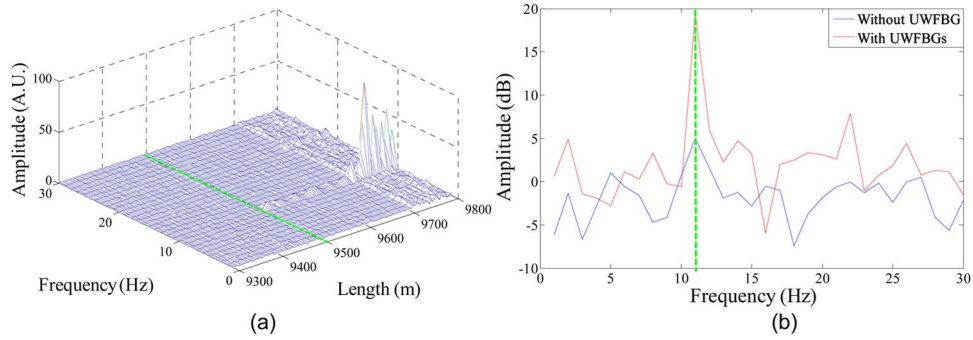
Fig. 10. Frequency spectra of vibrations. (a) Frequency spectra along the sensing fiber. (b) Frequency spectra at the positions with and without UWFBG.
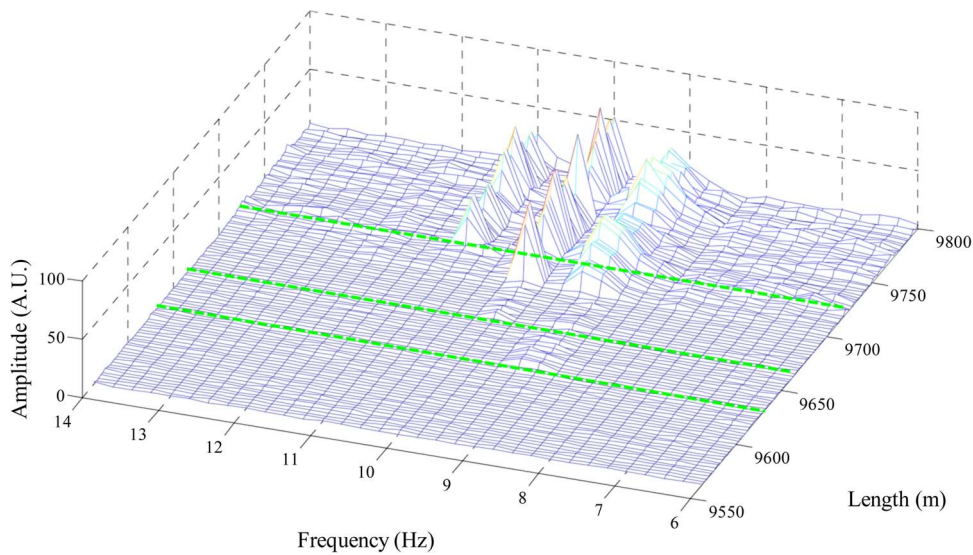

Fig. 11. Spectra along the sensing fiber when three vibrations were applied at different positions.

without UWFBGs were 12 dB and 3 dB, respectively, as shown in Fig. 10(b). Therefore, the SNR of the spectra was improved by about 9 dB combining the UWFBGs, which is a significantly improvement on vibration detection.

The response of the proposed system to multiple vibrations was also studied. In our experiment, three vibrations with frequency components of 9.2 Hz, 10 Hz, and 11 Hz were applied at 9630 m, 9665 m, and 9725 m, respectively. The time domain signals within 4 s were collected in the experiment. Therefore, the frequency resolution of this system was 0.25 Hz. The spectra along the sensing fiber were obtained as shown in Fig. 11. The spectra between 9630 m and 9665 m only have 9.25 Hz frequency component while the spectra between 9665 m and 9725 m contain 9.25 Hz and 10 Hz frequency components. Meanwhile, there are three frequency components (9.25, 10, and 11 Hz) in the spectra after 9725 m. Therefore, by comparing the spectra along the fiber, the position information of three vibrations can be easily obtained, achieving multiple vibrations distributed fiber sensing. Moreover, the SNR of the spectra in UWFBGs region (after 9700 m) are much larger than the SNR of spectra in non-UWFBGs region (before 9700 m), which proves that multiple vibrations sensing sensitivity are also improved by inducing UWFBGs. In the experiments, the sensitivity improvement of 9 Hz and 10 Hz frequency components are about 8.7 dB and 8 dB, respectively, which are closed to the sensitivity improvement of single vibration detection. In addition, the spectra before the third vibration position have no frequency

component related to 11 Hz especially the UWFBGs region (between 9700 m and 9725 m). Thus, the introduction of UWFBGs can be successfully used for vibrations detection sensitivity enhancement without bring detrimental effect on identifying the vibration's location, which is consistent with our results in simulation.

3.5. Discussion

In this paper, due to the limitation of experimental condition, only 10 UWFBGs have been fabricated and connected to the end of 9.7 km SMF sensing network. However, it has already proved the SNR and vibration detection sensitivity improvement of POTDR system in the experiment. Actually, UWFBGs can be fabricated over entire sensing fiber using existing on-line FBG fabrication technology, and then, the SNR and sensitivity enhancement at any position in a long-distance POTDR can be achieved. As the sensitivity enhancement is achieved in this work, weaker vibrations can be sensed. Hence, this enhanced sensing system can be used for the health and safety monitoring of large structures, perimeter security monitoring, geological safety monitoring, and so on.

When we increase the width of pulse, the SNR can be further improved. However, the spatial resolution would be reduced at this situation. Moreover, polarization fading would be induced with the pulse width increasing. Therefore, the chosen of pulse width and corresponding interval of UWFBGs for SNR further improvement needs further research. In addition, if the reflectivity of UWFBGs is increased, the insertion loss introduced by UWFBGs and the SNR enhancement would all be significant. Thus, it is difficult to visually judge whether the sensing length is increased or not. Although the relationship between the improved sensing length and the reflectivity of UWFBGs has been simulated in this work, the effect of UWFBGs' reflectivity and interval of UWFBGs on sensing length should be studied by experiments in future work.

4. Conclusion

In conclusion, a POTDR combined with UWFBG array system has been demonstrated theoretically and experimentally with significantly improved SNR and sensitivity for vibration and load sensing. The enhanced POTDR sensing system incorporating UWFBGs with reflectivity at only 1.1×10^{-5} has showed an improvement of 11 dB in SNR, in comparison with the traditional POTDR system, which also means the sensing distance is improved for about 27.5 km. Meanwhile, the load can be detected using POTDR system with 10.7 dB improved detection sensitivity. Moreover, distributed vibration detection can also be achieved by the enhanced system. Using the proposed system, vibration detection sensitivity can be improved by about 9 dB.

References

[1] A. J. Rogers, "Polarization optical time domain reflectometry: A technique for the measurement of field distributions," *Appl. Opt.*, vol. 20, no. 6, pp. 1060–1074, Mar. 1981.
[2] B. Huttner, B. Gisin, and N. Gisin, "Distributed PMD measurement with a polarization-OTDR in optical fibers," *J. Lightw. Technol.*, vol. 17, no. 10, pp. 1843–1848, Oct. 1999.
[3] H. Dong, P. Shum, Y. Gong, and Q. Sun, "Single-ended measurement of polarization dependent loss in an optical fiber link," *IEEE Photon. Technol. Lett.*, vol. 23, no. 3, pp. 185–187, Feb. 2011.
[4] F. Corsi, A. Galtarossa, and L. Palmieri, "Beat length characterization based on backscattering analysis in randomly perturbed single mode fibers," *J. Lightw. Technol.*, vol. 17, no. 7, pp. 1172–1178, Jul. 1999.
[5] Z. Zhang and X. Bao, "Distributed optical fiber vibration sensor based on spectrum analysis of polarization-OTDR system," *Opt. Exp.*, vol. 16, no. 14, pp. 10240–10247, Jul. 2008.
[6] N. Linze, P. Megret, and M. Wuilpart, "Development of an intrusion sensor based on a polarization-OTDR system," *IEEE Sens. J.*, vol. 12, no. 10, pp. 3005–3009, Oct. 2012.
[7] M. E. Fermann, S. B. Poole, D. N. Payne, and F. Martinez, "Comparative measurement of Rayleigh scattering in single mode optical fibers based on an OTDR technique," *J. Lightw. Technol.*, vol. 6, no. 4, pp. 545–551, Apr. 1988.
[8] J. Hu *et al.*, "Photon-counting optical time-domain reflectometry using superconducting nanowire single photon detector," *J. Lightw. Technol.*, vol. 30, no. 16, pp. 2583–2587, Aug. 2012.
[9] D. Lee *et al.*, "SNR enhancement of OTDR using birothogonal codes and generalized inverse," *IEEE Photon. Technol. Lett.*, vol. 17, no. 1, pp. 163–165, Jan. 2005.

[10] D. Lee, H. Yoon, P. Kim, J. Park, and N. Park, "Optimization of SNR improvement in the noncoherent OTDR based on simplex codes," *J. Lightw. Technol.*, vol. 24, no. 1, pp. 322–328, Jan. 2006.

[11] Z. Qin, L. Chen, and X. Bao, "Continuous wavelet transform for nonstationary vibration detection with phase-OTDR," *Opt. Exp.*, vol. 20, no. 18, pp. 20 459–20 465, Aug. 2012.

[12] K. O. Hill *et al.*, "Chirped in-fiber Bragg gratings compensation of optical fiber dispersion," *Opt. Lett.*, vol. 19, no. 17, pp. 1314–1316, Sep. 1994.

[13] P. Petropoulos, M. Ibsen, M. N. Zervas, and D. J. Richardson, "Generation of a 40 GHz pulse stream by pulse multiplication with a sampled fiber Bragg grating," *Opt. Lett.*, vol. 25, no. 8, pp. 521–523, Apr. 2000.

[14] G. A. Ball and W. H. Glenn, "Design of a single mode linear cavity Erbium fiber laser utilizing Bragg reflectors," *J. Lightw. Technol.*, vol. 10, no. 10, pp. 1338–1343, Oct. 1992.

[15] Y. Feng, L. R. Taylor, and D. B. Calia, "150 W highly efficient Raman fiber laser," *Opt. Exp.*, vol. 17, no. 26, pp. 23 678–23 683, Dec. 2009.

[16] K. O. Hill and G. Meltz, "Fiber Bragg grating technology fundamentals and overview," *J. Lightw. Technol.*, vol. 15, no. 8, pp. 1263–1274, Aug. 1997.

[17] W. Zhang, X. Dong, Q. Zhao, G. Kai, and S. Yuan, "FBG-type sensor for simultaneous measurement of force (or displacement) and temperature based on bilateral cantilever beam," *IEEE Photon. Technol. Lett.*, vol. 13, no. 12, pp. 1340–1342, Dec. 2001.

[18] Y.-L. Lo and S.-H. Xu, "New sensing mechanisms of an optical time domain reflectometry with fiber Bragg gratings," presented at the Opt. Fiber Sens. Conf., Cancun, Mexico, 2006, paper TuE4.

[19] M. Zhang *et al.*, "A large capacity sensing network with identical weak fiber Bragg gratings multiplexing," *Opt. Comm.*, vol. 285, no. 13/14, pp. 3082–3087, Jun. 2012.

[20] C. G. V. Luiz *et al.*, "Time and wavelength multiplexing of fiber Bragg grating sensor using commercial OTDR," in *Proc. OFS*, Portland, OR, USA, May 2003, pp. 151–154.

[21] I. Kuo and Y. Chen, "In-service OTDR monitoring supported fiber Bragg grating optical add-drop multiplexers," *IEEE Photon. Technol. Lett.*, vol. 14, no. 6, pp. 867–869, Jun. 2002.

[22] Y. Rao, Z. Ran, and R. Chen, "Long-distance fiber Bragg grating sensor system with a high optical signal-to-noise ratio based on a tunable fiber ring laser configuration," *Opt. Lett.*, vol. 31, no. 18, pp. 2684–2686, Aug. 2006.

[23] Y. Wang *et al.*, "A large serial time division multiplexed fiber Bragg grating sensor network," *J. Lightw. Technol.*, vol. 30, no. 17, pp. 2751–2756, Sep. 2012.

[24] M. Han, Y. Wang, and A. Wang, "Grating-assisted polarization optical time-domain reflectometry for distributed fiber-optic sensing," *Opt. Lett.*, vol. 32, no. 14, pp. 2028–2030, Jul. 2007.

[25] C. Fabrizio, G. Andrea, and P. Luca, "Polarization mode dispersion characterization of single mode optical fiber using backscattering technique," *J. Lightw. Technol.*, vol. 16, no. 10, pp. 1832–1843, Oct. 1998.

[26] M. Wuilpart, P. Megret, M. Blondel, A. J. Rogers, and Y. Defosse, "Measurement of the spatial distribution of birefringence in optical fibers," *IEEE Photon. Technol. Lett.*, vol. 13, no. 8, pp. 836–838, Aug. 2001.